Optik 98, No. 1 (1994) 15–20

Theta microscopy allows phase regulation in 4Pi(A)-confocal two-photon fluorescence microscopy

S. Lindek [+]*, N. Salmon [+], C. Cremer*, E. H. K. Stelzer [+]

[+] Light Microscopy Group, European Molecular Biology Laboratory (EMBL), Heidelberg, Germany
* Institut für Angewandte Physik, Universität Heidelberg, Germany

Theta microscopy allows phase regulation in 4Pi(A)-confocal two-photon fluorescence microscopy. A solution for the phase problem in 4Pi(A)-confocal fluorescence microscopy has been found by observation orthogonal to the optical axis. Three-dimensional intensity distributions for 4Pi(A)-confocal microscopy and confocal theta microscopies are calculated. The evaluations in the focal region show that the volume integrals of the 4Pi(A)-point spread functions are strongly attenuated when the interference is not constructive in the geometrical focus. This results in a phase dependent fluorescence intensity signal with a modulation of up to 48% with which the relative phase of the interfering wavefronts can be measured and regulated.

Theta-Mikroskopie ermöglicht Phaseneinstellung bei 4Pi(A)-konfokaler Zweiphotonen-Fluoreszenzmikroskopie. Eine Lösung des Phasenproblems der 4Pi(A)-konfokalen Fluoreszenzmikroskopie ist die Beobachtung der Probe senkrecht zur optischen Achse. Dreidimensionale Intensitätsverteilungen sind für 4Pi(A)-konfokale Mikroskope und konfokale Theta-Mikroskope berechnet worden. Die Auswertung im Fokalbereich zeigt, daß das Raumintegral der 4Pi(A)-Punktbildfunktion stark verringert wird, wenn die Interferenz im geometrischen Fokus nicht konstruktiv ist. Dadurch ergibt sich ein phasenabhängiges Fluoreszenzintensitätssignal mit einer Modulation von bis zu 48%, mit der die relative Phase der interferierenden Wellenfronten bestimmt und geregelt werden kann.

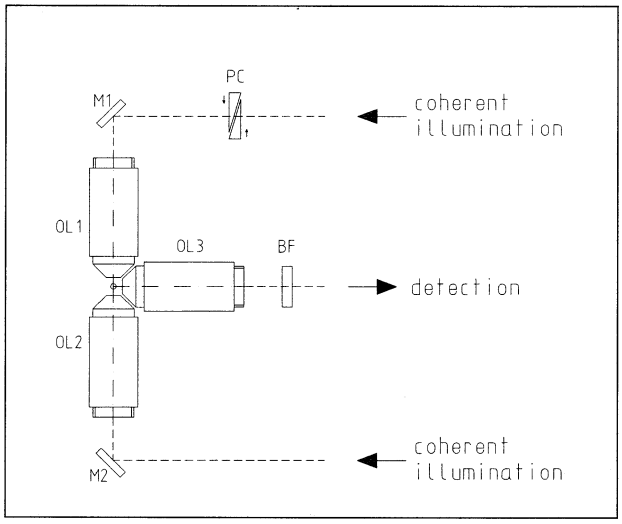

Fig. 1. Simplified drawing of the 4Pi(A)-confocal theta microscope. Three lenses (OL1, OL2, OL3) are arranged with a common focus. The sample is coherently illuminated from opposite directions through OL1 and OL2 and the orthogonal emission is detected with OL3. A phase compensator (CP) is used to adjust the phase of the illumination light. A barrier filter (BF) blocks the excitation laser light.

1 Introduction

In light microscopy the intensity distribution in the focal region of the objective lens is described by the coherent amplitude point spread function (PSF) $h(x, y, z)$. In confocal fluorescence microscopy the PSF is the product of the illumination and detection intensity PSFs. The confocal PSF is therefore more confined to the focus than the PSF in a conventional microscope. This is equivalent to an increase in resolution [1–4]. A further resolution enhancement can be achieved by decreasing the wavelength used for illumination or for detection, increasing the numerical aperture of the optical system, or applying theta microscopy, i.e. observing the fluorescence emission at an angle ϑ to the optical axis [5, 6].

4Pi-confocal microscopy increases the aperture and therefore improves the axial resolution of a confocal microscope [7, 8]. This has been demonstrated experimentally for both fluorescence light microscopy and scattered light microscopy [7, 9]. However these investigations have shown that the resolution increase cannot be exploited for the observation of e.g. biological material since 4Pi-confocal microscopy has to deal with two problems: Firstly, it uses interference to increase the axial resolution through a sub-structured PSF. This results in a main maximum accompanied by further maxima of lower intensity along the optical axis. These axial side lobes are responsible for about half of the observed intensity [7]. Secondly, the interference pattern depends on the phase difference of the interfering waves, and the localisation of the emission centres in the sample can only be improved over confocal microscopy if the phase difference is controlled.

Recently, a new microscopic arrangement called theta microscopy has been proposed. This arrangement improves the axial resolution by a factor of 3.5 without the use of interference [5, 6]. In theta microscopy two or more objective lenses are used to illuminate the sample and to collect its fluorescence emission. The resolution enhancement stems from the alignment of the lenses: the detection axis is tilted by an angle ϑ relative to the illumination axis. If ϑ is 90°, the overlap of the illumination and detec-

Received March 22, 1994.

Steffen Lindek, Nick Salmon, Ernst H. K. Stelzer, Light Microscopy Group, European Molecular Biology Laboratory (EMBL), Postfach 102209, D-69012 Heidelberg.

Christoph Cremer, Institut für Angewandte Physik, Universität Heidelberg, Albert-Überle-Straße 3–5, D-69120 Heidelberg.

tion PSFs and hence their product, which is the confocal theta PSF, are minimised. The small extent of the confocal theta PSF is equivalent to high axial and lateral resolutions. A combination of theta and 4Pi(A)-confocal microscopy has been described by Stelzer and Lindek [5]. In 4Pi(A)-confocal theta microscopy the sample is illuminated as in 4Pi(A)-confocal microscopy and the emitted light is detected through an orthogonally oriented objective lens (fig. 1). Detection perpendicular to the illumination axis rejects the side lobes of the 4Pi-illumination PSF, and the resulting PSF becomes almost spherical. This solves the problem of the axial side lobes in 4Pi(A)-confocal microscopy and leads to the best three-dimensional resolution yet published.

In this paper we show that the rejection of the axial side lobes of the 4Pi-illumination PSF in 4Pi(A)-confocal theta two-photon fluorescence microscopy is so efficient that it is sensitive to the regulation of the phase of the interfering wavefront. The intensity that can be detected by orthogonal observation is much higher when the sample is illuminated with constructive interference in the geometrical focus than when illuminated with destructive interference. To document this intensity variation we present an analytical theory of the intensity signals that can be recorded for various three-dimensional confocal and confocal theta PSFs, and the results of a "brute force" numerical analysis of the PSFs.

2 Analytical theory

The intensity PSF $|h_{cf}(x, y, z)|^2$ of a confocal fluorescence light microscope is given by the product of the illumination and detection intensity PSFs:

$$|h_{cf}(x, y, z)|^2 = |h_{\mathrm{ill}}(x, y, z)|^2 \, |h_{\mathrm{det}}(x, y, z)|^2 . \tag{1}$$

x, y, z is a set of Cartesian coordinates with z corresponding to the optical axis. In a 4Pi(A)-confocal microscope the illumination PSF is sub-structured by an interference pattern, which can be taken account of by a $\cos^2$-term in the case of single-photon fluorescence:

$$\begin{aligned} |h_{4\mathrm{Pi}}(x, y, z, k, \phi)|^2 &= |h_{4\mathrm{Pi,\,ill}}(x, y, z, k, \phi)|^2 \, |h_{\mathrm{det}}(x, y, z)|^2 \\ &= |h_1(x, y, z) \exp(i(kz + \phi)) \\ &\quad + h_2(x, y, -z) \\ &\quad \cdot \exp(-i(kz + \phi))|^2 \, |h_{\mathrm{det}}(x, y, z)|^2 \\ &= |h_{\mathrm{ill}}(x, y, z)|^2 \, |h_{\mathrm{det}}(x, y, z)|^2 \\ &\quad \cdot \cos^2(kz + \phi) . \end{aligned} \tag{2}$$

$k = 2\pi n/\lambda$ is the wave number, n is the refractive index of the medium in the focal region and λ is the illumination wavelength. ϕ is the phase difference of the interfering wavefronts. In the case of two-photon absorption the illumination PSF of the system is given by the single-photon PSF squared [8, 10]. This means that the exponent of the cosine-modulation term changes to 4.

The intensity signal I detected in a confocal fluorescence microscope is found by integrating the confocal or 4Pi-confocal PSF:

$$I = \int_{-\infty}^{\infty} \int_{-\infty}^{\infty} \int_{-\infty}^{\infty} |h_{cf/4\mathrm{Pi}}(x, y, z, k, \phi)|^2 \, dx\, dy\, dz . \tag{3}$$

In the vicinity of the focus the PSF is nearly symmetric with respect to all three axes and the mixed terms become very small in a confocal setup. Thus they can be neglected and the integral can be separated:

$$I \approx \int_{-\infty}^{\infty} \int_{-\infty}^{\infty} |h_{cf}(x)|^2 \, |h_{cf}(y)|^2 \, dx\, dy \int_{-\infty}^{\infty} |h_{cf/4\mathrm{Pi}}(z, k, \phi)|^2 \, dz . \tag{4}$$

The first integral is a constant factor which is not affected by the character of the confocal PSF. $|h_{cf/4Pi}(z, k, \phi)|^2$ can be approximated by a Gaussian and in the case of 4Pi-illumination the modulation term is as described in eq. (2). The total intensity for single-photon fluorescence is thus:

$$I_{1hv}(\sigma_1, k, \phi) = A_1 \int_{-\infty}^{\infty} \exp\left(-\frac{z^2}{2\sigma_1^2}\right) \cos^2(kz + \phi) \, dz \tag{5a}$$

and for two-photon fluorescence:

$$I_{2hv}(\sigma_2, k, \phi) = A_2 \int_{-\infty}^{\infty} \exp\left(-\frac{z^2}{2\sigma_2^2}\right) \cos^4(kz + \phi) \, dz \tag{5b}$$

where σ_1 and σ_2 are the standard deviations of the intensity distribution along the z-axis for single-photon and two-photon fluorescence respectively.

For single-photon fluorescence this integral yields:

$$I_{1hv}(\sigma_1, k, \phi) = A_1 \sqrt{\frac{\pi}{2}}\, \sigma_1 \frac{\exp(2(k\sigma_1)^2) + \cos(2\phi)}{\exp(2(k\sigma_1)^2)} \tag{6a}$$

and for two-photon absorption:

$$\begin{aligned} I_{2hv}(\sigma_2, k, \phi) = A_2 \sqrt{\frac{\pi}{2}}\, \sigma_2 \Bigg[&\frac{3}{4} + \frac{\cos(2\phi)}{\exp(2(k\sigma_2)^2)} \\ &+ \frac{\cos(4\phi)}{4\exp(8(k\sigma_2)^2)} \Bigg] . \end{aligned} \tag{6b}$$

The functions I_{1hv} and I_{2hv} can be normalized to 1 for $\phi = 0$, thus yielding:

$$\hat{I}_{1hv}(\sigma_1, k, \phi) = \frac{\exp(2(k\sigma_1)^2) + \cos(2\phi)}{\exp(2(k\sigma_1)^2) + 1} \tag{7a}$$

and

$$\hat{I}_{2hv}(\sigma_2, k, \phi) = \frac{3\exp(8(k\sigma_2)^2) + 4\exp(6(k\sigma_2)^2)\cos(2\phi) + \cos(4\phi)}{3\exp(8(k\sigma_2)^2) + 4\exp(6(k\sigma_2)^2) + 1} . \tag{7b}$$

The functions $\hat{I}_{1hv}$ and $\hat{I}_{2hv}$ are parametric functions of the phase ϕ. The parameters are k and σ_1 or σ_2, which depend on the extent of the PSF along the z-axis.

The intensity variation with phase (eqs. (7a) and (7b)) was calculated for water immersion objective lenses with a numerical aperture (NA) of 0.94. Such a numerical aperture is equivalent to an aperture angle of 45°, the maxi-

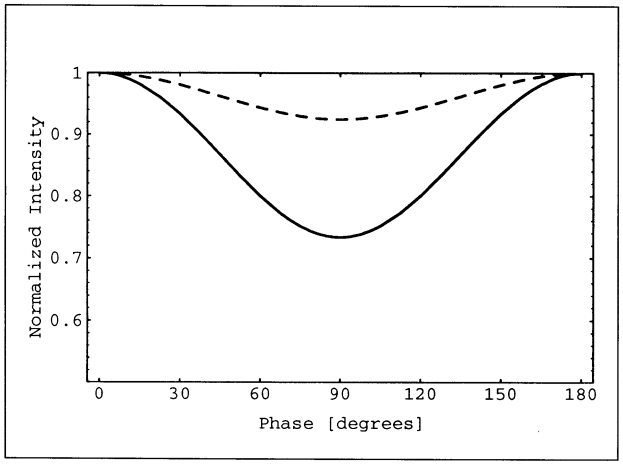

Fig. 2. Dependence of the intensity signal on the phase difference in a 4Pi(A)-confocal theta microscope with two-photon absorption (λ_{ill} = 780 nm and λ_{det} = 430 nm). The data is calculated with the analytical expression. The dashed line is for NA = 0.75, the solid line is for NA = 0.94.

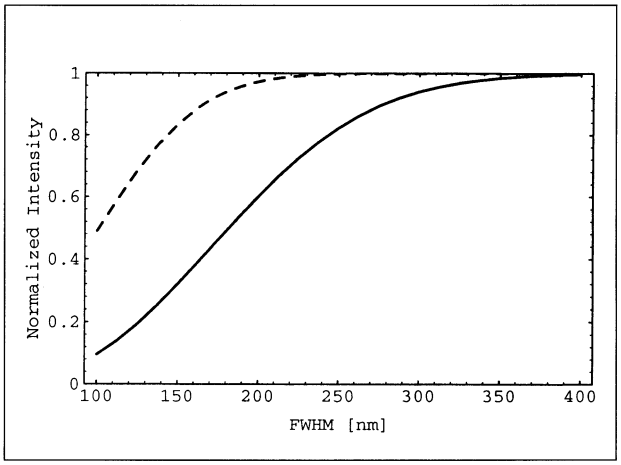

Fig. 3. Dependence of the intensity signal for $\phi = \pi/2$ on the FWHM in a 4Pi(A)-confocal theta microscope. The dashed line represents the maximal modulation for single-photon fluorescence (λ_{ill} = 488 nm and λ_{det} = 520 nm), the solid line for two-photon fluorescence (λ_{ill} = 780 nm and λ_{det} = 430 nm).

mum possible with the confocal theta setup shown in fig. 1. Unfortunately, such lenses are not available yet and hence we have also performed the same calculation for NA = 0.75 which is the numerical aperture of a lens obtainable from Zeiss (Germany). The parameters σ_1 and σ_2 were calculated using the full width half-maxima (FWHM) ($\sigma_{1,2}$ = FWHM/2.36) derived by Stelzer and Lindek [5] for these numerical apertures and for the illumination and detection wavelengths for FITC [11] (λ_{ill} = 488 nm and λ_{det} = 520 nm) in the single-photon fluorescence case and for Coumarin 138 [11] (λ_{ill} = 780 nm and λ_{det} = 430 nm) in the two-photon fluorescence case.

In the case of single-photon fluorescence the phase dependent intensity variation is below 0.1% both for NA = 0.75 and for NA = 0.94. The intensity modulation for two-photon fluorescence, which follows a periodicity of π, is displayed in fig. 2. The modulation is 8% for NA = 0.75 and 27% for NA = 0.94.

These results suggest that the excitation wavelength in single-photon fluorescence is so short compared with the FWHM of the PSF and thus the interference maxima are so close together that a large part of the interference pattern is always detected by theta observation. To test this dependence of the fluorescence intensity signals of the FWHM the confocal theta PSF was evaluated for both single- and two-photon fluorescence. Fig. 3 shows the modulation depth of the intensity signal for FWHMa between 100 and 400 nm. The FWHM can be varied e.g. through the numerical aperture of the system.

3 Numerical theory

The numerical calculation of the three-dimensional PSFs is based on the scalar theory that is described in Born and Wolf [12] and that has also been applied for the evaluation of confocal theta PSFs by Stelzer and Lindek [5]. This scalar theory is correct for aperture angles below 50° [13] and therefore adequate for the aperture angles used in these calculations.

In this paper all PSFs are calculated in Cartesian coordinates that originate in the geometrical focus. In this theory, no assumptions concerning the symmetry of the PSFs were made. The three-dimensional PSFs can be characterised by several methods, e.g. by their FWHMa along the coordinate axes. We chose two criteria: firstly, the intensity signal was evaluated by calculating the volume integral of the PSF (eq. (3)). Secondly, the volume enclosed by an isosurface of the PSF provided an estimation of the observation volume. It was calculated by the integration of all volume elements that had an intensity value above a given threshold of 0.5 or 0.1 for normalized PSFs. Note that the normalisation of 4Pi-PSFs requires division not simply by the PSF's maximum, but by the value of the PSF at the geometrical focus with constructive interference.

The three-dimensional PSFs were evaluated under the same conditions as described above. The intensity distribution was calculated within a cube of $1.2 \times 1.2 \times 1.2$ μm^3 around the geometrical focus thus ensuring that only intensity values that are so small as to be insignificant are not taken into account.

The results of the numerical evaluation of the PSFs for single-photon fluorescence showed no significant phase dependent intensity modulation and are therefore not presented here. The results for confocal, confocal theta, 4Pi(A)-confocal and 4Pi(A)-confocal theta two-photon microscopy are summarised in tables 1 (NA = 0.94) and 2 (NA = 0.75). The 4Pi-PSFs were evaluated for constructive interference in the focus. For each intensity distribution two observation volumes, the percentage of the total intensity enclosed in these volumes and the intensity integrated over the total volume of 1.73 μm^3 are present-

Table 1. Characterisation of point spread functions in confocal two-photon fluorescence microscopies. All data is calculated for NA = 0.94 in water, λ_{ill} = 780 nm and λ_{det} = 430 nm. The 4Pi-PSFs are evaluated for constructive interference in the geometrical focus.

NA = 0.94	observation volume enclosed by 50%-intensity isosurface [10^6 nm^3]	percentage of total intensity in 50%-observation volume [%]	observation volume enclosed by 10%-intensity isosurface [10^6 nm^3]	percentage of total intensity in 10%-observation volume [%]	total intensity signal (normalised to confocal)
confocal	14.3	32.7	79.5	84.9	1.00
confocal theta	6.6	31.0	35.8	79.5	0.48
4Pi(A)-confocal	2.9	17.4	30.4	76.2	0.36
4Pi(A)-confocal theta	3.1	30.2	17.6	78.7	0.24

Table 2. Characterisation of point spread functions in confocal two-photon fluorescence microscopies. All data is calculated for NA = 0.75 in water, λ_{ill} = 780 nm and λ_{det} = 430 nm. The 4Pi-PSFs are evaluated for constructive interference in the geometrical focus.

NA = 0.75	observation volume enclosed by 50%-intensity isosurface [10^6 nm^3]	percentage of total intensity in 50%-observation volume [%]	observation volume enclosed by 10%-intensity isosurface [10^6 nm^3]	percentage of total intensity in 10%-observation volume [%]	total intensity signal (normalised to confocal)
confocal	37.8	42.9	148.3	89.7	1.00
confocal theta	13.5	31.7	73.3	81.3	0.48
4Pi(A)-confocal	8.1	25.4	56.5	79.3	0.34
4Pi(A)-confocal theta	5.0	30.1	28.3	78.4	0.19

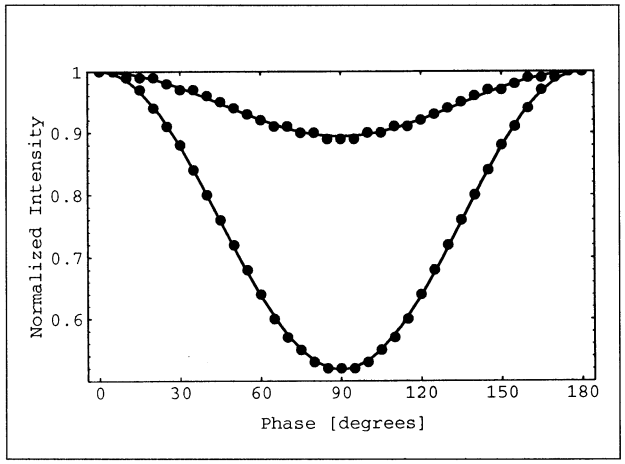

Fig. 4. Dependence of the intensity signal on the phase difference in a 4Pi(A)-confocal theta microscope with two-photon absorption. The dots represent the numerically computed data with λ_{ill} = 780 nm and λ_{det} = 430 nm. The graphs show the non-linearly fitted curves, computed with the analytical expression of eq. (7b). The upper graph is for NA = 0.75, the lower graph is for NA = 0.94.

ed. These tables document the spatial resolution of 4Pi(A)-confocal and theta microscopies and provide three-dimensionally evaluated data that goes beyond the results given in ref. [5].

Fig. 4 shows the results of the numerical evaluation of the phase dependence of the intensity signal for NA = 0.75 and 0.94 in a 4Pi(A)-confocal theta microscope working with two-photon absorption. It demonstrates a modulation of up to 48%.

To illustrate this phase dependence, fig. 5 displays the intensity distribution for constructive (a) and for destructive (b) interference in the geometrical focus for a 4Pi(A)-confocal microscope working with NA = 0.94. Fig. 6 shows analogous PSFs for a 4Pi(A)-confocal theta microscope. Fig. 6a shows that theta microscopy suppresses the side lobes along the illumination axis in the case of constructive interference. This stems from the suppression by theta observation. Fig. 6b shows the intensity distribution after a phase shift of $\phi = \pi/2$ and documents that the two main maxima of the normalised interference pattern are reduced to values of about 0.3 which results in a total intensity of 48% below the value for $\phi = 0$.

4 Discussion

The 50%-observation volumes in tables 1 and 2 show the resolution improvement by theta two-photon microscopy: in a confocal microscope the three-dimensional resolution is improved by a factor 2 or 3; a 4Pi(A)-confocal theta microscope even improves the resolution by a factor of 5 or 7. The progress due to theta microscopy is higher when working with lower numerical apertures as these result in very elongated PSFs that can be efficiently reduced in extent by detecting orthogonally to the optical axis (table 2).

Care must be taken when considering the 50%-observation volumes in 4Pi(A)-confocal microscopy (2.9 10^6 nm^3 for NA = 0.94 and 8.1 10^6 nm^3 for NA = 0.75) since the axial lobes are mainly taken into account only in the 10%-observation volume. The percentage of total intensity that is included in the respective observation volume documents the focusing quality of the system: the higher the percentage is, the better the light is focused onto a single spot. Consequently the 4Pi(A)-confocal microscope shows very low values (e.g.

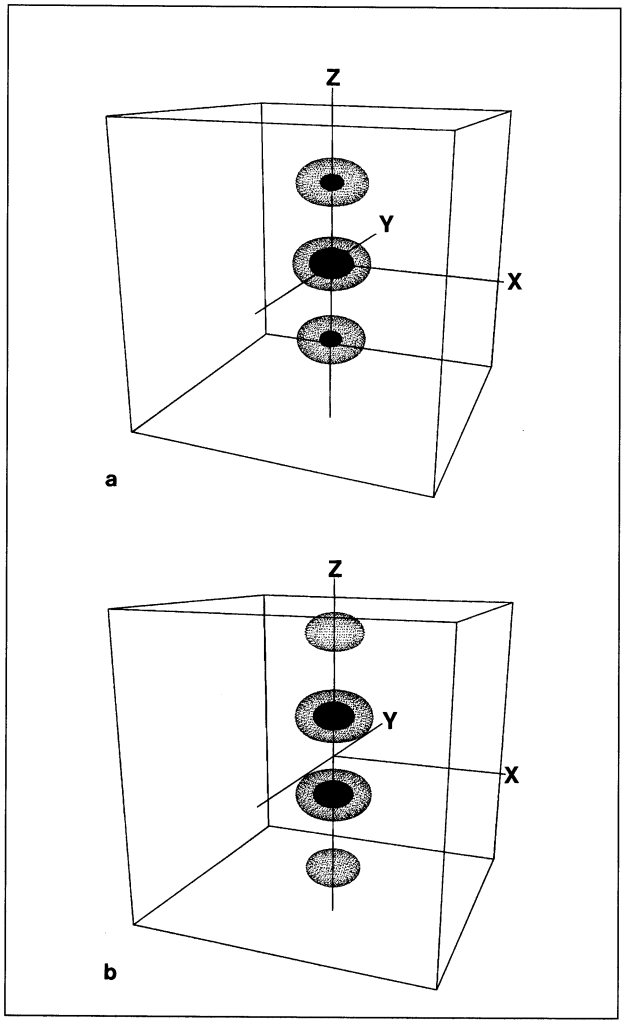

Fig. 5. Pi(A)-confocal point spread functions. All data is calculated numerically for NA = 0.94 in water and two-photon fluorescence with λ_{ill} = 780 nm and λ_{det} = 430 nm. Isosurface plots at 50% (solid) and 10% (dotted) of the normalised PSFs are shown for a) constructive interference, b) destructive interference in the geometrical focus. Both illumination and detection are performed along the z-axis. The volume surrounded by the grid is 1.2^3 µm^3 large.

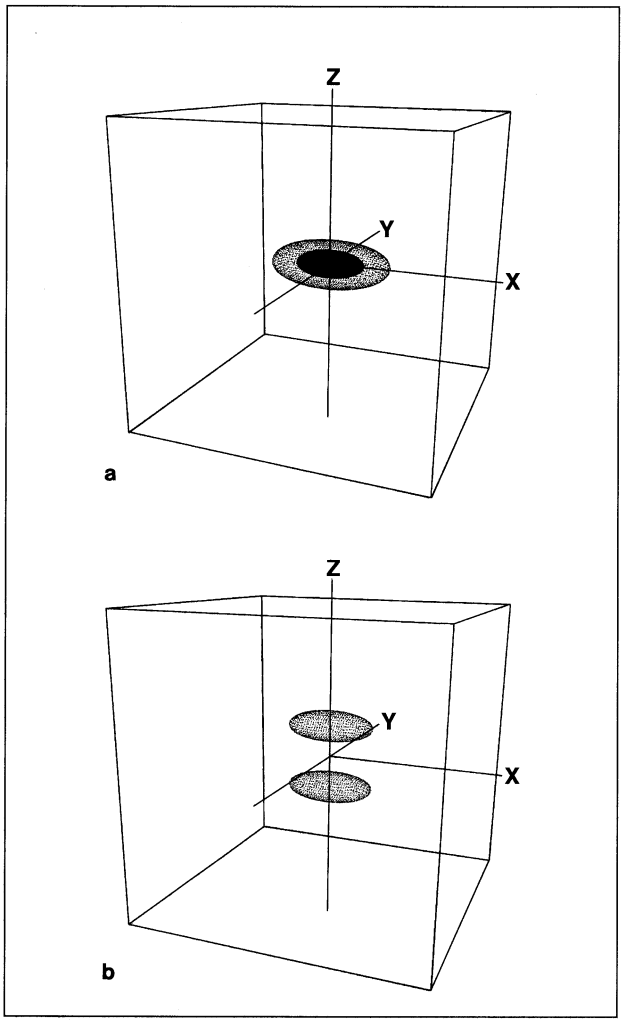

Fig. 6. 4Pi(A)-confocal theta point spread functions. All data is calculated numerically for NA = 0.94 in water and two-photon fluorescence with λ_{ill} = 780 nm and λ_{det} = 430 nm. Isosurface plots at 50% (solid) and 10% (dotted) of the normalised PSFs are shown for a) constructive interference, b) destructive interference in the geometrical focus. z is the illumination axis and x is the detection axis. The volume surrounded by the grid is 1.2^3 µm^3 large.

17% for NA = 0.94). This loss in well-focused intensity has to be added to the intensity loss of the total system, which is documented in the last column: e.g. in a 4Pi(A)-confocal two-photon microscope only a third of the fluorescence intensity of a confocal system is detected (in the single-photon case 50% of the intensity is detected in a 4Pi(A)-confocal setup).

The discrepancy between the analytical and numerical evaluations of the basic integral in eq. (3) can be mainly explained by the broadening of the interference pattern due to focusing effects [7]. This effect positively influences the phase modulation calculated analytically. A non-linear fit of the analytical expression of eq. (7b) to the numerical data of fig. 4 gives a broadening of 5.4% for NA = 0.75 and 22.7% for NA = 0.94. The fitted curves are both displayed in fig. 4. The numbers for the broadening are consistent since we expect a smaller wavenumber for the high numerical aperture case. Furthermore the curvature of the interference pattern which is due to the numerical aperture [7, 8] is neglected when applying the analytical theory and can also affect the resulting numerical values.

In summary, we have shown that the phase problem, which is the main difficulty when realising a 4Pi-confocal microscope, can be solved by theta observation. This method shows good results if used with objective lenses with a high numerical aperture and with two-photon absorption. In an experiment the intensity modulation with phase angle can be used to ensure constructive interference in the 4Pi-microscope. Additionally, the effect can

be used to measure the coherence length of the illumination light and to equalise the illumination paths. The combination of different numerical apertures for the 4Pi-illumination objective lenses and for the orthogonal detection lens could possibly bring an improvement of the phase dependent modulation of the intensity. Also the effect of an apodisation of the lenses with annular apertures (which leads to a smaller extent of the detection PSF and thus may increase the phase sensitivity) has to be investigated.

Acknowledgements

The authors would like to thank R. Pick for his support. S. L. would like to thank the Boehringer Ingelheim Fonds for supporting his research work. Mathematica [14] was used for the analytical calculations and several figures. The remaining figures were calculated using AVS (AVS Inc., Waltham, Ma., USA).

References

[1] C. J. R. Sheppard, A. Choudhury: Image formation in the scanning microscope. Optica Acta **24** (1977) 1051–1073.

[2] G. J. Brakenhoff, P. Blom, P. Barends: Confocal scanning light microscopy with high aperture immersion lenses. J. Microsc. **117** (1979) 219–232.

[3] I. J. Cox, C. J. R. Sheppard, T. Wilson: Super-resolution by confocal fluorescent microscopy. Optik **60** (1982) 391–396.

[4] T. Wilson, C. J. R. Sheppard: Theory and Practice of Scanning Optical Microscopy. pp. 37–78. Academic Press, London 1984.

[5] E. H. K. Stelzer, S. Lindek: Fundamental reduction of the observation volume in far-field light microscopy by detection orthogonal to the illumination axis: confocal theta microscopy. Opt. Commun., in press.

[6] S. Lindek, E. H. K. Stelzer: Confocal theta microscopy and 4Pi-confocal theta microscopy. SPIE Proc. **2184** (1994) 188–194.

[7] S. Hell, E. H. K. Stelzer: Properties of a 4Pi-confocal fluorescence microscope. J. Opt. Soc. Am. A **9** (1992) 2159–2166.

[8] S. Hell, E. H. K. Stelzer: Fundamental improvement of resolution with a 4Pi-confocal fluorescence microscope using two-photon excitation. Opt. Commun. **93** (1992) 277–282.

[9] S. W. Hell, S. Lindek, C. Cremer, E. H. K. Stelzer: Measurement of the 4Pi-confocal point spread function proves 75 nm axial resolution. Appl. Phys. Lett. **64** (1994) 1335–1337.

[10] E. H. K. Stelzer, S. Hell, S. Lindek, R. Stricker, R. Pick, C. Storz, G. Ritter, N. Salmon: Nonlinear absorption extends confocal fluorescence microscopy into the ultraviolet regime and confines the illumination volume. Opt. Commun. **104** (1994) 223–228.

[11] Kodak: Optical Products. Rochester, USA.

[12] M. Born, E. Wolf: Principles of Optics. pp. 370–458. Pergamon Press, Oxford 1980.

[13] H. H. Hopkins: The airydisk formula for systems of high relative aperture. Proc. Phys. Soc. **55** (1943) 116.

[14] S. Wolfram: Mathematica – A system for doing mathematics by computer. Addison-Wesley, Redwood City 1991.